DE-FC22-95BC14942--08

Advanced Reservoir Characterization and Evaluation of C02 Gravity Drainage in the Naturally Fractured Sprayberry Trend Area

Quarterly Report
January 1 - March 31, 1998

By:
David S. Schechter

Work Performed Under Contract No.: DE-FC22-95BC14942

For
U.S. Department of Energy
Office of Fossil Energy
Federal Energy Technology Center
P.O. Box 880
Morgantown, West Virginia 26507-0880

By
Petroleum Recovery Research Center
New Mexico Institute of Mining and Technology
Socorro, New Mexico 87801

Disclaimer

PRRC Report No. 98-19

Quarterly Technical Report

ADVANCED RESERVOIR CHARACTERIZATION AND EVALUATION OF CO_2 GRAVITY DRAINAGE IN THE NATURALLY FRACTURED SPRABERRY TREND AREA

DOE Contract No.: DE-FC22-95BC14942

New Mexico Petroleum Recovery Research Center
New Mexico Institute of Mining and Technology
Socorro, New Mexico 87801
(505) 835 5142

Contract Date:	September 1, 1995
Anticipated Completion Date:	September 1, 2000
Program Manager:	Paul McDonald Pioneer Natural Resources USA, Inc.
Principal Investigator:	David S. Schechter New Mexico Petroleum Recovery Research Center
Contracting Officer's Representative:	Jerry F. Casteel National Petroleum Technology Office
Report Period:	January 1, 1998 - March 31, 1998

US/DOE Patent Clearance is not required prior to the publication of this document.

ABSTRACT

The overall goal of this project is to assess the economic feasibility of CO_2 flooding the naturally fractured Spraberry Trend Area in west Texas. This objective is being accomplished by conducting research in four areas: 1) extensive characterization of the reservoirs, 2) experimental studies of crude oil/brine/rock (COBR) interaction in the reservoirs, 3) analytical and numerical simulation of Spraberry reservoirs, and, 4) experimental investigations on CO_2 gravity drainage in Spraberry whole cores. This report provides results of the first quarter of 1998 in the third area.

The CO_2 flooding project is going into Phase II, i.e., Field Demonstration. Pilot scale reservoir simulation for the CO_2 flooding is necessary for both initial pilot design and design modification in the future. In order to perform a quality simulation study with a dual porosity reservoir simulator, it is vitally important to use reliable reservoir parameters as input data. In the first quarter of 1998, we conducted investigations on refinement of reservoir parameters to be used in the pilot scale simulation of CO_2 flooding the naturally fractured Spraberry Trend Area reservoir. We concluded that the absolute permeability of the rock matrix to be input into the dual porosity simulator should be the permeability determined from drainage oil-water capillary pressure curve rather than air permeability, water permeability, or oil permeability. The secondary porosity and the on-trend fracture permeability have been estimated using a simple mathematical model based on fracture characterization data. The results are consistent with that derived from well test analyses and are being verified using coreflood data and a newly developed scaling model presented in this document.

TABLE OF CONTENTS

LIST OF TABLES AND FIGURES

EXECUTIVE SUMMARY

The goal of this project is to test the economic feasibility of CO_2 injection in the naturally fractured Spraberry Trend Area in the Permian Basin. CO_2 injection in naturally fractured reservoirs does not meet classic screening criteria due to the expectation of excessive channeling of low viscosity CO_2 through the natural fractures. However, the number of naturally fractured reservoirs and the low recovery usually attendant with these reservoirs combined with abundance of natural CO_2 sources strongly suggests the necessity of exploring counter-intuitive process options. The success of a CO_2 pilot in the naturally fractured Midale reservoir fortified by laboratory experiments performed under the Department of Energy's Extraction Technology Program were the driving force behind the undertaking of such a risky venture. Both lab and field results indicated that injection of IFT-lowering gas could result in gravity drainage of oil in the matrix blocks if the fractures had sufficient vertical relief and significant density.

The CO_2 flooding project is in Phase II, i.e., Field Demonstration. In order to optimize the design and maximize the performance of the CO_2 flood pilot, pilot scale reservoir simulation for the CO_2 flooding is necessary. To perform a quality simulation study with a dual porosity reservoir simulator, it is vitally important to use reliable reservoir parameters as input data. In the first quarter of 1998, theoretical investigations were conducted on refinement of reservoir parameters to be used in the pilot scale simulation of CO_2 flooding the naturally fractured Spraberry Trend Area reservoir. We concluded that the absolute permeability of the rock matrix to be input into the dual porosity simulator should be the permeability determined from drainage oil-water capillary pressure curve rather than air permeability, water permeability, or oil permeability. We also concluded that the secondary porosity and on-trend fracture permeability can be estimated using a newly developed mathematical model based on data from fracture characterization. The results are consistent with that derived from well test analyses and are being verified by scaling up the coreflood data obtained using cores with representative natural fractures. Such a scaling model is also presented in this study.

INTRODUCTION

Three-phase, three-dimensional, dual-porosity reservoir simulation is a useful tool for analyzing performance of dual-porosity oil reservoirs. However, it is generally recognized that history matching is more difficult in simulation of dual-porosity reservoirs, as more input parameters are required and the parameters are usually not easy to determine. Among many of the parameters are primary permeability, secondary porosity and permeability, and permeability anisotropy. Rough data input into the simulator results in high uncertainties in reservoir performance predictions, which is the traditional GIGO (garbage-in garbage-out) problem. This document describes a new approach to determination of some of the input parameters for simulation of CO_2 flooding the naturally fractured Spraberry Trend Area reservoir in west Texas.

The results of this investigation demonstrate that the primary permeability, or the absolute matrix permeability, to be used in the simulator should be determined from the oil-water drainage capillary pressure curve. Although core flood performance provides a good estimate of matrix porosity, permeability derived from the core flood depends strongly upon fluid type in low permeability region due to wetting behavior of the rock. The matrix permeability estimated from water-oil capillary pressure is more realistic for reservoir simulation. Water-oil capillary pressure should be from direct measurements or scaled from mercury injection results if interfacial tension and contact angle data are available. The secondary porosity due to natural fractures has been estimated based on the average fracture intensity and aperture. Fracture intensity and aperture were determined from horizontal core retrieved from the E.T. O'Daniel No. 28. The secondary permeability due to natural fractures has been estimated based on a parallel flow mathematical model. The results are consistent with that derived from well test analyses and are being verified by scaling up core flood data obtained using reservoir cores from the naturally fractured Spraberry Trend Area. The scaling model is presented in this report.

ABSOLUTE MATRIX PERMEABILITY

The absolute matrix permeability of a porous medium is a term that students learn from their first reservoir engineering class. Although this term is familiar to all reservoir engineers, appropriate application of the parameter in multiphase flow analysis is not so obvious. The absolute matrix permeability is theoretically a property of the porous medium itself, not fluids in the pore. This means that the same absolute permeability should be measured for a given porous medium regardless of fluid type used in the measurement. This is essentially true for high permeability media. However, it has been found that the absolute permeability depends strongly on fluid properties in low permeability media. For example, Table 1 shows air, water, and oil permeabilities of 10 core samples taken from the Spraberry Trend Area reservoir. The dependence of the absolute permeability on fluid properties is interpreted to be due to wettability of the porous material to different fluids. The effect of wetting behavior on fluid transport is less significant in large pores, whereas major fluid volumes flow far from the pore wall where wetting effects dominate resistance to flow. This effect is more significant in small pores where fluid flows near the pore wall.

The fact is that the air permeability, water permeability, and oil permeability are all true absolute permeabilities for the flow of the three individual phases. A question then arises: Which absolute permeability should one use in the reservoir simulation? To answer this question, it is necessary to examine the flow process that needs to be simulated. It is known that multiphase flow exists and water is the draining phase in miscible CO_2 flooding. Since CO_2 is miscible with oil in the reservoir, water-oil drainage capillary pressure should dominate pressure-flow rate relations during the displacement process. Thus, the absolute matrix permeability should be estimated from the water-oil drainage capillary pressure curve.

Relationship between Capillary Pressure and Rock Permeability

Capillary pressure curves have long been used in petroleum industry for analyzing behavior of oil reservoirs.[1,2] Much information about porous materials, such as pore size distribution, can be obtained based on capillary pressure curves.[3] The currently used methods for determination of rock permeabilities from capillary pressure curves are essentially based on the work by Purcell.[4] By combination of Poiseuille's equation and Darcy's Law for a hypothetical porous medium composed of a large number of parallel, cylindrical capillaries of equal length, Purcell proposed the following equation:

$$k = 2F\phi\sigma^2 \cos^2\theta \int_0^1 P_c^{-2} dS_b \tag{1}$$

where k is permeability, F is a lithology factor accounting for differences between flow in the hypothetical porous medium and that in naturally occurring rocks, σ is interfacial tension, θ is contact angle, ϕ is porosity, P_c is capillary pressure, and S_b is non-wetting phase saturation as a fraction of bulk volume.

Thomeer[5] found that when the capillary pressure and saturation data are plotted on a log-log paper, a smooth, best-fit curve approximates a hyperbola, which is mathematically expressed as follows:

$$\log(P_c / P_d) \;\; \log(S_b / S_{b\sim}) = -C^2 \tag{2}$$

where P_d is displacement pressure (threshold), $S_{b\sim}$ is non-wetting phase saturation at infinitive capillary pressure, C^2 is a pore geometrical factor. Thomeer also plotted air permeability against $S_{b\sim}/P_d$ on log-log paper for constant C values. Linear relationship was observed from the plots. No explanation was given in Thomeer's paper about why such a linear relationship exists.

Swanson[6] presented a simple correlation between permeabilities and mercury capillary pressures based on the shape of the initial-residual curve. It was found that the curve bends at initial saturations greater than about 0.42. The point of the bend of the curve was considered to be an indication of transition from broadening spacial distribution and trapping to fine structure trapping and intrusion of the non-wetting phase into corners of pores. With no knowledge of where the bend corresponds to on a general capillary pressure curve, Swanson chose point "A"

through which a 45° tangent line can be drawn as an approximation. Because the ratio of non-wetting phase saturation to the capillary pressure at the point A, $(S_b/P_c)_A$ is maximal and easy to identify graphically, Swanson chose the ratio as a parameter for relating capillary pressure curve to permeability. Values of the parameter $(S_b/P_c)_A$ were determined on 319 sandstone and carbonate samples representing 74 formations using the tangent approach. A linear relation between $(S_b/P_c)_A$ and air (and brine) permeability was observed. Based on the linear relation, Swanson presented a homograph for estimating brine permeabilities from capillary pressure curves.

Walls and Amaefule[7] applied Swanson's parameter $(S_b/P_c)_A$ for tight gas sands. They developed a linear correlation between $(S_b/P_c)_A$ and permeability similar to, but better than Swanson's correlation in the low permeability (<0.1 md) region. Because the Swanson's procedure requires the construction of 45° lines tangent to the capillary pressure curve in order to define $(S_b/P_c)_A$, Walls and Amaefule found it difficult to generate $(S_b/P_c)_A$ automatically using a computer routine. They therefore developed a new procedure for ease of computer generation of the parameter $(S_b/P_c)_A$. The new procedure involves tabulating, or plotting, $(P_c/S_b)^{1/2}$ versus S_b data. A minimum value, $(P_c/S_b)_{min}^{1/2}$, can be found from the plot for each sample. The Swanson parameter $(S_b/P_c)_A$ can then determined with the following equation.

$$(S_b / P_c)_A^{-1/2} = (P_c / S_b)_{\min}^{1/2} \tag{3}$$

However, Walls and Amaefule[7] did not provide any proof of Eq. (3). It is believed that Eq. (3) was established based on the fact that S_b/P_c is at a maximum at point A, as stated by Swanson. This equation will be proven in the next section.

Analytical Determination of Swanson Parameter $(S_b/P_c)_A$

Swanson's parameter $(S_b/P_c)_A$ is very useful in estimating rock permeability from capillary pressure data. However, as shown by Walls and Amaefule,[7] the graphic procedure presented by Swanson[6] for determination of the parameter is time consuming. Walls and Amaefule's[7] tabulating/graphic procedure is also not convenient to use in computerized analysis. It is desirable to develop a simple equation for calculation of the parameter. Derivation of such an equation can be done if capillary pressure data can be fit to Eq. (2). In fact, the equation of the 45° line passing through the origin of the hyperbola represented by Eq. (2) can be expressed as follows in the log-log P_c-S_b scale:

$$\log(P_c / P_d) = -\log(S_b / S_{b\sim}) \tag{4}$$

where the negative sign comes from the slope of the line. Combination of Eqs. (2) and (4) gives the solution of coordinates at the intersection between the capillary pressure curve and the 45 degree line (point "A" in Swanson's paper) as follows:

$$S_{bA} = 10^C S_{b\sim} \tag{5}$$

and

$$P_{cA} = 10^{-C} P_d \tag{6}$$

Dividing Eq. (5) by Eq. (6) yields a simple expression for Swanson's parameter:

$$(S_b / P_c)_A = 10^{2C} (S_{b\sim} / P_d) \tag{7}$$

Eq. (7) can also be derived based on the fact that S_b/P_c is maximal (P_c/S_b is minimal) at point A as shown below.

Eq. (2) gives:

$$P_c = P_d 10^{-C^{2/\log(S_b/S_{b\sim})}} \tag{8}$$

Dividing Eq. (8) by S_b yields:

$$P_c / S_b = 10^{-C^{2/\log(S_b/S_{b\sim})}} P_d / S_b \tag{9}$$

Let $f(S_b) = P_c / S_b$. It can be shown that

$$\frac{\partial f}{\partial S_b} = 10^{-C^{2/\log(S_b/S_{b\sim})}} P_d / S_b{}^2 \left\{ \frac{C^2}{\left[\log(S_b / S_{s\sim})\right]^2} - 1 \right\} \tag{10}$$

Since $f(S_b)$ is minimal at point A, application of $\frac{\partial f}{\partial S_b} = 0$ to Eq. (10) and solving for S_b gives:

$$S_{bA} = 10^C S_{b\sim} \tag{11}$$

and

$$P_{cA} = 10^{-C} P_d \tag{12}$$

Dividing Eq. (11) by Eq. (12) yields a simple expression for Swanson's parameter:

$$(S_b / P_c)_A = 10^{2C} (S_{b\sim} / P_d) \tag{13}$$

which is identical to Eq. (7). This also proves that Walls and Amaefule's[7] tabulating/graphic method for determining the Swanson parameter is valid.

Advantages of Using Eq. (13)

The first advantage of using Eq. (13) for determination of Swanson parameter is simplicity. This is due to the simple form of the equation. Compared to Swanson's graphic procedure and Walls' tabulating/graphic procedure, Eq. (13) is much easier to use in computerized calculations. The second advantage of using Eq. (13) is the accuracy of the result compared to Swanson's graphic procedure and Walls and Amaefule's[7] tabulating/graphic procedure where significant error can result from reading coordinates of the point A from a log-log plot. For example, for the capillary pressure data presented in Fig. 1b in Swanson's paper,[6] the Swanson parameter is determined to be 0.48 based on Swanson's graphic procedure, while Eq. (13) gives a value of 0.47. For the capillary pressure data shown in Fig. 4 in Swanson's paper[6] (Fig. 1 in Walls and Amaefule's paper[7]), the Swanson parameter is determined to be 0.61 based on Swanson's graphic procedure, while Eq. (13) gives a quite low value of 0.44.

Application of Eq. (13) to the Spraberry Sand

A match between the oil-water drainage capillary pressure for a Spraberry core and Eq. (2) is shown in Fig. 1. This match gives the following parameters for the Spraberry sand:

$$C = 0.24$$

$$S_b = 0.098$$

$$P_d = 7 \text{ psig.}$$

The Swanson's parameter can then be determined based on Eq. (13):

$$(S_b / P_c)_A = 0.042 .$$

Swanson[6] proposed the following correlation for determination of water permeability:

$$k_w = 431\left(\frac{S_b}{P_c}\right)_A^{2.109} \qquad (14)$$

Substituting $(S_b / P_c)_A = 0.042$ into Eq. (14) results in

$$k_w = 0.538 \text{ md}$$

which should be used as the absolute matrix permeability in the simulation of waterflooding in Spraberry Trend Area reservoirs.

SECONDARY POROSITY

The secondary porosity, ϕ_f , due to natural fractures may be estimated based on the average fracture aperture and fracture spacing using a simple relation:

$$\phi_f = \frac{w}{S_f} \tag{15}$$

where w and S_f are fracture aperture and spacing respectively. As discussed in our Second Annual Report,[8] the average fracture aperture in the Spraberry Trend Area may be taken as 0.0025 inch. Based on recent fracture characterization,[8] three distinct fracture sets, trending NNE, NE, and ENE, are present in cores from the 1U and 5U units in the Upper Spraberry zone. The average fracture spacing of the three fracture sets are 1.62, 3.17, and 3.79 feet, respectively. Since the three sets of natural fractures co-exist in reservoir pay zones, the distance between natural fractures in all sets must be lower than 1.62 ft. In fact the distances between most of the NNE fractures are less than 1 ft. If we assume that the average distance between the inter-set of natural fractures is 0.5 ft (or 6 inches), substituting w = 0.0025 inch and S_f = 6 inches into Eq. (15) yields ϕ_f = 0.0004. Well testing[9,10] has not clearly demonstrated dual porosity pressure transient behavior in the Spraberry Trend. This indicates that fracture volume is less than 1/1000 of the matrix volume,[11] which is consistent with the low value of ϕ_f estimated here.

SECONDARY PERMEABILITY

The secondary permeability due to natural fractures is also called fracture permeability in well test models and dual-porosity simulators. However, it is different from the fracture permeability that frequently used in hydraulic stimulation analysis where the hydraulically induced, proppant-filled fracture is treated as a porous medium that has an intrinsic permeability. The fracture permeability for a hydraulically induced fracture is a property of the fracture itself, while the secondary permeability due to natural fractures is a defined parameter for the fracture network and its magnitude depend on both fracture conductivity and fracture intensity. In the following analyses, these two permeabilities are distinguished using terms *secondary permeability* k_s and *intrinsic fracture permeability* k_f. These two parameters differ by a factor that equals the secondary porosity as shown in this section.

The secondary permeability is the highest in the fracture on-trend direction and the lowest in the fracture off-trend direction. The permeability anisotropy may be estimated based on well testing data as shown in our Second Annual Report.[8] Here we present two approaches for estimating the on-trend secondary permeability. This first one is called parallel flow model, and the second one is referred to as the scaling model.

Parallel Flow Model

Assuming parallel flow in the fracture and matrix, a simple interrelationship between the effective on-trend reservoir permeability, matrix permeability, and intrinsic fracture permeability has been derived (see Appendix A for details):

$$k_e = (1-\phi_f)k_m + \phi_f k_f \tag{16}$$

where k_e, k_m, and k_f are the on-trend effective reservoir permeability, matrix permeability, and intrinsic fracture permeability, respectively. The second term in the right-hand-side of Eq. (16) is the secondary permeability k_s in the on-trend direction:

$$k_s = \phi_f k_f \tag{17}$$

We can estimate the intrinsic fracture permeability in the on-trend direction using the following expression:[8]

$$k_f = \frac{\varphi_f{}^3 w^2}{12} \tag{18}$$

where φ_f is the fracture porosity accounting for volume of minerals, crushed rock, and proppant introduced during hydraulic fracturing operations.

Mineralized fractures were found in the 1U unit of the Upper Spraberry[8] with an average percentage of mineral-filling in the fractures of about 75%. Hairline fractures found in the 5U unit of the Upper Spraberry are not mineralized. If we assume the fracture porosity to be about 0.25, substituting φ_f = 0.25 and w = 0.0025 inch into Eq. (18) results in

$$k_f = 78{,}125 \text{ md.}$$

The secondary permeability in the on-trend direction can then estimated using Eq. (17):

$$k_s = (0.0004)\ (78{,}125) = 31 \text{ md}$$

which is very close to the on-trend fracture permeability derived from well testing analyses.[8]

Scaling Model

If the permeability of a core plug with representative natural fractures is measured, the secondary permeability can also be estimated using a scaling model presented hereafter. The interrelationship between plug permeability k_p, intrinsic fracture permeability k_f, and fracture conductivity K_f is given by:

$$k_p \frac{\pi d^2}{4} = k_f hw = K_f h \tag{19}$$

where d and h are plug diameter and total fracture length measured in the cross sectional area of the plug, respectively. Solving the left part of Eq. (19) for k_f yields:

$$k_f = k_p \frac{\pi d^2}{4hw}. \tag{20}$$

Substituting Eqs. (15) and (20) into Eq. (17) gives

$$k_s = k_p \frac{\pi d^2}{4hS_f}. \tag{21}$$

If fracture conductivity, rather than plug permeability, is measured, the intrinsic fracture permeability can be determined by solving the right part of Eq. (19) for k_f:

$$k_f = \frac{K_f}{w}. \tag{22}$$

Substituting Eqs. (15) and (22) into Eq. (17) gives

$$k_s = \frac{K_f}{S_f}. \tag{23}$$

It is important to note that fracture aperture w, a parameter that is difficult to measure, does not appear in Eqs. (21) and (23), which makes the two equations easy to use. We are currently measuring the k_p using a Spraberry core plug with natural fractures to test the validity of Eq. (21).

SUMMARY

The CO_2 flooding project is entering Phase II, i.e., the Field Demonstration. Pilot scale reservoir simulation for CO_2 flooding is necessary for both initial pilot design and design modification in the future. In order to perform a quality simulation study with a dual porosity reservoir simulator, it is vitally important to use reliable reservoir parameters as input data. In the first quarter of 1998, we conducted investigations on refinement of reservoir parameters to be used in the pilot scale simulation of CO_2 flooding. We concluded that the absolute permeability of the rock matrix to be input into the dual porosity simulator should be the permeability determined from drainage oil-water capillary pressure curve rather than air permeability, water permeability, or oil permeability. Its value is 0.538 md. We also concluded that the secondary porosity and the on-trend secondary permeability due to natural fractures can be estimated using a simple mathematical model based on fracture characterization data. Their values in the Spraberry Trend Area are estimated to be 0.0004 and 31 md respectively. These numbers are consistent with that

estimated from well test interpretation[8] and are being verified using experimental data and a scaling model.

REFERENCES

1. Leverett, M.C.: “Capillary Behavior in Porous Solids,” *Trans*. AIME (1941) **142**, 151.
2. Leverett, M.C., Lewis, W.B. and True, M.E.: “Dimensional Model Studies of Oil Field Behavior,” *Trans*. AIME (1942) **146**, 175.
3. Ritter, H.L. and Drake, L.C.: **“**Pore Size Distribution in Porous Materials,” *Ind. and Eng. Chem.* (1945) **17**, 782.
4. Purcell, W.R.: “Capillary Pressures—Their Measurement Using Mercury and the Calculation of Permeability Therefrom,” *Trans*. AIME (1949) **186**, 39.
5. Thomeer, J.H.M.: “Introduction of a Pore Geometrical Factor Defined by the Capillary Pressure Curve,” *J. Pet. Tech*. (March 1960) 73-77.
6. Swanson, B.F.: “A Simple Correlation Between Permeabilities and Mercury Capillary Pressures,” *J. Pet. Tech*. (December 1981) 2498-2504.
7. Walls, J.D. and Amaefule, J.O.: “Capillary Pressure and Permeability Relationships in Tight Gas Sands,” paper SPE 13879 presented at the SPE Low Permeability Reservoirs Symposium held in Denver, Colorado, May 19-22, 1985.
8. Schechter, D.S.: “Advanced Reservoir Characterization and Evaluation of CO_2 Gravity Drainage in the Naturally Fractured Spraberry Trend Area,” Second Annual Technical Progress Report, U.S. DOE Contract No. DE-FC22-95BC14942 (Dec 1997).
9. Baker, R.: “Pressure Test Analysis for Midkiff 25-08,” (April 1994) PRRC Spraberry Database.
10. Baker, R.: “Vertical Pulse Test Analysis of Shackelford 1-38A,” (April 1994) PRRC Spraberry Database.
11. Van Golf-Racht, D.T.: *Fundamentals of Fractured Reservoir Engineering*, Elsevier Scientific Publishing Co., New York, 1982.

Appendix A - Interrelationship between Effective On-Trend Reservoir Permeability, Matrix Permeability and Intrinsic Fracture Permeability in Naturally Fracture Reservoirs

A simple relationship between effective on-trend reservoir permeability, matrix permeability and intrinsic fracture permeability in naturally fracture reservoirs can be analytically established based on an assumption of parallel flow in matrix and fracture.

Consider a fractured porous medium shown in Fig. 2. If the pressure drop across the length L is ΔP, according to Darcy’s law, the total flow rate Q of a fluid with viscosity μ is expressed as

$$Q = \frac{k_e A \Delta p}{\mu L} \quad \text{(A.1)}$$

where k_e and A are the effective permeability and total cross sectional area, respectively. If we use k_m and A_m to denote matrix permeability and matrix cross sectional area respectively, the flow rate through the matrix body Q_m is expressed as

$$Q_m = \frac{k_m A_m \Delta p}{\mu L} \quad \text{(A.2)}$$

Similarly, if we denote intrinsic fracture permeability and fracture cross sectional area by k_f and A_f respectively, the flow rate through the fractures Q_f is expressed as

$$Q_f = \frac{k_f A_f \Delta p}{\mu L} \quad \text{(A.3)}$$

Since

$$Q = Q_m + Q_f \quad \text{(A.4)}$$

Substitutions of Eqs. (A.1), (A.2) and (A.3) into Eq. (A.4) yield

$$k_e = \frac{A_m}{A} k_m + \frac{A_f}{A} k_f \quad \text{(A.5)}$$

Since

$$A = A_m + A_f \quad \text{(A.6)}$$

and

$$\phi_f = \frac{A_f}{A} \quad \text{(A.7)}$$

where ϕ_f is the secondary porosity due to fracture, Eq. (A.5) is rewritten as

$$k_e = (1 - \phi_f) k_m + \phi_f k_f \quad \text{(A.8)}$$

Equation (A.8) represents a general relationship between the effective on-trend reservoir permeability, matrix permeability and intrinsic fracture permeability in naturally fracture reservoirs.

In most oil and gas reservoirs ϕ_f is much less than 1. Equation (A.8) thus degenerates to

$$k_e = k_m + \phi_f k_f \quad \text{(A.9)}$$

This equation indicates that intrinsic fracture permeability linearly contributes to the effective on-trend reservoir permeability with a proportionality factor of ϕ_f , the secondary porosity due to the fractures.

The first term in Eq. (A.9) for matrix permeability is usually much smaller than the second term. The effective on-trend reservoir permeability is thus dominated by intrinsic fracture permeability:

$$k_e \approx \phi_f k_f \,. \qquad \text{(A.10)}$$

It can be shown that the secondary porosity ϕ_f due to fracture relates to the fracture width (aperture) w and fracture spacing S_f through the following equation:

$$\phi_f = \frac{w}{S_f} \,. \qquad \text{(A.11)}$$

Therefore, if w and S_f are estimated from fracture characterization and k_f is measured on core plugs, the secondary porosity and the effective on-trend reservoir permeability k_e can be estimated from Eq. (A.10). This effective on-trend reservoir permeability may be compared with the on-trend effective permeability derived from well tests.

Table 1 - Air, Water, and Oil Permeabilities of Spraberry Trend Area Reservoir Cores

Core Sample No.	Porosity (%)	Absolute Permeability (md)		
		Air	Water	Oil
SP-1	10.0	0.43	0.28	0.09
SP-2	10.1	0.45	0.22	0.10
SP-3	9.80	0.44	0.23	0.14
SP-4	10.0	0.46	0.14	0.06
SP-5	10.7	0.49	0.27	0.09
SP-6	9.85	0.43	0.22	
SP-7	10.4	0.34	0.20	0.08
SP-10	12.8	0.36	0.15	0.05

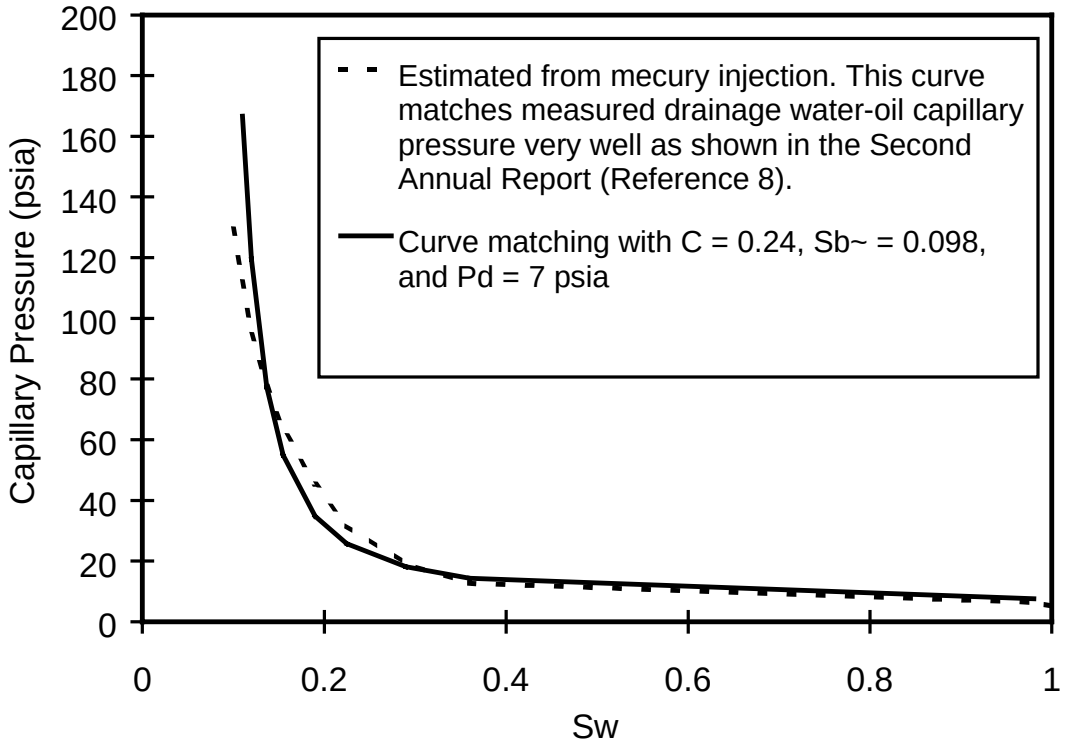

Fig. 1 - Curve matching of oil-water drainage capillary pressure for a Spraberry core

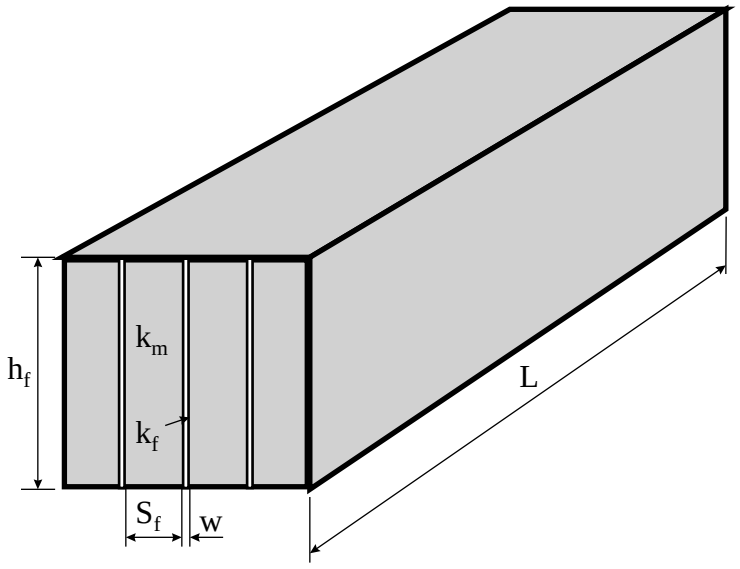

Fig. 2 - A parallel-flow model for simulating fluid flow in naturally fractured reservoirs.